

# Embedded-Cluster Study of Hydrogen Interaction with an Oxygen Vacancy at the Magnesium Oxide Surface

Annalisa D'Ercole, Elio Giamello, and Cesare Pisani\*

*Dipartimento di Chimica IFM, Università di Torino, and Unità INFM di Torino,  
via Giuria 5, I-10125 Torino, Italy*

Lars Ojamäe

*Department of Physical Chemistry, Arrhenius Laboratory, Stockholm University, 10691 Stockholm, Sweden*

*Received: January 8, 1999*

An embedded-cluster Hartree–Fock approximation is adopted for simulating the formation of  $F_s(H)$  color centers at the (001) surface of magnesium oxide. This process is assumed to take place in two steps at an isolated surface anion vacancy: first, a hydrogen molecule is adsorbed dissociatively at the defect; second, following UV irradiation, a neutral hydrogen atom is removed and an electron remains trapped at the vacancy with a hydroxyl group nearby. According to the present calculations, the activation energy for the dissociation is appreciable (about 25 kcal/mol) and the products (a proton bound to a low-coordinated oxygen and a hydride ion above the vacancy) are considerably less stable than the reactants. The excitation of the adsorbed species owing to the UV irradiation is simulated by considering a singlet–triplet transition of the hydride–vacancy complex, which then dissociates into an H atom and a trapped lone electron. The electronic structure and the EPR parameters of the resulting paramagnetic state are explored. The theoretical results agree in many respects with the experimental data as concerns one of the forms of heterolytically dissociated hydrogen which are found at the defective MgO surface. However, from the viewpoint of the energetics, this model is untenable because that species is known to form irreversibly at room temperature with low activation energy.

## 1. Introduction

In spite of its long history, the problem of the characterization of the surface of MgO is still a subject of active research. Important experimental information is currently obtained through the combined use of ultraviolet (UV), infrared (IR), and electron paramagnetic resonance (EPR) spectroscopies, both in the absence and in the presence of an adsorbed species. In the case of hydrogen adsorption, after the first observation of the unusual phenomenon of heterolytic splitting at the MgO surface,<sup>1</sup> subsequent detailed studies have shown that two different families of dissociated hydrogen are formed, to be indicated in the following as  $\alpha$  and  $\beta$ . The first corresponds to an  $H^+ - H^-$  pair weakly bound at the surface (its concentration is pressure-dependent and vanishes upon evacuation) and the second to an analogous pair which however is irreversibly held at the surface at room temperature.<sup>2,3</sup> Both species have been carefully characterized by IR spectroscopy: the  $H^+$  species is stabilized at the surface as a hydroxyl group, while  $H^-$  is adsorbed at cationic sites. It is worth noting that in the  $\alpha$  family the hydride appears as a linearly adsorbed species, while the  $\beta$  hydride is in a bridged configuration. For the formulation of suitable models of such kind of experimental findings, theoretical calculations are becoming an important complementary tool. In a recent paper which summarizes the experience of many years of research in this field and utilizes new data obtained with all the above-mentioned tools, one of us (E.G.) has formulated a novel model for the  $F_s^+(H)$  color center, an EPR active species which is known to be formed at the surface of fully dehydrated MgO in the presence of hydrogen and after UV activation.<sup>3</sup> According to this hypothesis, to be cited in the

following as the vertex model, the trapped electron is localized at a site formed by three magnesium cations at a micro(111) face of the sample (in the limiting case, at the vertex of a one-layer terrace on the (100) face). It contrasts with the more traditional one, formulated long ago by Tench<sup>4,5</sup> and re-explored recently by several authors,<sup>6–10</sup> according to which the electron trap consists of an oxygen vacancy at the (001) face. The divacancy model proposed by Lunsford<sup>11,12</sup> is still another possibility which has been the object of recent work.<sup>13</sup> With respect to these older hypotheses, the vertex model appears in better agreement with the experimental evidence concerning the surface chemistry of hydrogen on MgO and some features of the color center, in particular as concerns the modification of the EPR spectrum after oxygen adsorption. Furthermore, it does not require the energetically expensive formation of an oxygen vacancy at the flat (001) surface. An important aspect of the analysis carried out in that study is the recognition that the formation of the  $F_s^+(H)$  center upon UV activation takes place in parallel with the disappearance of the hydride species, especially with that belonging to the  $\alpha$  family; the hydride is therefore considered to be the source of the trapped electron.

In the present paper we consider, from a theoretical viewpoint, the problem of the formation of the  $F_s^+(H)$  center. In order to keep the computational burden within reasonable limits, we take a step back and treat the case where hydrogen is adsorbed at an isolated surface anion vacancy. From the vertex model, however, we take the suggestion that a crucial role in the formation of the active species is played by a pre-existing hydride ion. We then consider explicitly the process of the heterolytic dissociation of the molecule at the vacancy, to form the *precursor state* of

the  $F_s^+(H)$  center, which consists in a hydride-like species above the vacancy and a hydroxyl group at a low-coordinated oxygen nearby. Because of its configuration, this precursor state appears to be related to the  $\beta$  rather than to the  $\alpha$  family of dissociated molecules. The hydride–vacancy complex resembles for some aspects a gas-phase  $H_2$  molecule and is indicated in the following as HV. The UV irradiation which is known to promote the formation of the paramagnetic species is here supposed to excite the HV complex to an unstable triplet state, resulting finally in a neutral hydrogen atom away from the center plus an electron trapped in the vacancy and a hydroxyl group in its vicinity: the *final state*. While the model here adopted for the formation of the  $F_s(H)$  center does not correspond to the more recent hypothesis, the present study can cast some light on the mode of hydrogen dissociation and excitation at defects. Furthermore, though possibly in low concentration because of its high energetic cost, the surface anion vacancy is certainly one of the typical defects which are present at the surface of alkali-earth oxides, and it is worthwhile to assess its chemical activity.

For the present simulations we have used a Hartree–Fock (HF) embedded-cluster approach as employed in our preceding studies of the anion vacancy<sup>10</sup> and divacancies.<sup>13</sup> We make reference to those articles and to the literature cited there for a detailed description of the method, based on the *perturbed-cluster* (PC) theory, and of the approximations adopted in the computer code EMBED which solves the PC equations.<sup>14</sup> According to this technique, a solution is first obtained for the defect-free semi-infinite MgO crystal (the host system), which is here simulated with a 4-layer slab parallel to the (001) face. A cluster is then selected, sufficiently large to accommodate all important chemical effects associated with the creation of the defect (removal of an oxygen ion, relaxation of nearby ions, addition of the hydrogen atoms, redistribution of the electron charge, etc.). The cluster solution is obtained after including in the cluster Hamiltonian the interaction with the remainder of the host system and is corrected for coupling the local wave function with that of the rest of the system; the whole procedure is repeated until self-consistency is achieved. It is then clear why the simulation of an isolated anion vacancy is computationally easier than that of the vertex model which corresponds to a more drastic departure from the perfect (001) crystal face.

Less sophisticated approaches have been adopted in previous simulations of hydrogen dissociation at the MgO surface.<sup>15–17</sup> In their pioneering studies on the surface chemistry of oxides, Colbourn and Mackrodt also considered hydrogen chemisorption on MgO.<sup>15</sup> Using very rough models (miniclusters surrounded by point charges) they found that dissociation does not take place at the perfect surface but occurs at different types of defects, in particular at the anion vacancy, with negligible activation energy. The use of cluster models in this kind of investigations can be exemplified by the work by Kobayashi et al.<sup>17</sup> who simulated the interaction of  $H_2$  with a local surface structure containing three-coordinated ions by employing a cubic ( $Mg_4O_4$ ) cluster. Among other adsorption processes, the heterolytic dissociation was studied and found to occur with no barrier; the adsorption energy was 37 kcal/mol at an HF level of approximation and reduced to 18.5 kcal/mol using second-order perturbation theory. We believe that these studies are not very significant for the problem we are presently addressing either because the approximations adopted are too drastic (see below) or because the situation described has nothing to do with the isolated surface anion vacancy.

Figure 1 shows the embedded clusters used for the present study; it also provides the equilibrium geometries for the

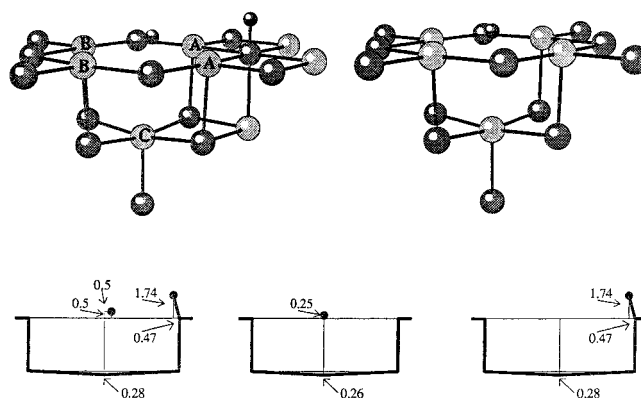


**Figure 1.** Embedded clusters used for studying the dissociation of the  $H_2$  molecule and the  $F_s^+(H)$  center (left) and the hydride–vacancy complex (right). Oxygen and magnesium ions are represented by dark and light gray circles, respectively, and hydrogens by small black circles. Labels on the Mg ions closest to the vacancy serve for the discussion of EPR data (see section para). The plots below report the respective equilibrium geometries (distances in Bohr): from left to right, the dissociated molecule at the surface, the hydride–vacancy complex, the  $F_s^+(H)$  center.

precursor and the final state, to be discussed in sections 2.B and 2.D. The high-quality basis set adopted for describing the host crystal atoms is as in the preceding work.<sup>10,13</sup> For hydrogen we have used a 31G\* basis set (two independent s orbitals plus polarization  $p$  functions). A set of floating single Gaussian functions (four of type  $s$ , one of type  $p$ ) centered at the location of the missing oxygen has been associated with the vacancy in order to allow the description of the trapped electron.<sup>10</sup> Problems arise when hydrogen approaches the surface to form the HV complex because the centers of the respective basis functions come close to each other leading to quasi-linear dependence problems. In this case the center of the floating Gaussians has been displaced down, so as to keep its distance from hydrogen 1.75 Bohr at least. The simulation of the excited triplet state of the complex has been effected by exploiting a facility of the EMBED code, which allows us, in the frame of the unrestricted Hartree–Fock (UHF) scheme, to populate selected cluster orbitals with a single electron of a given spin.

In the next section we present and discuss the results of our calculations, by adding, when needed, further computational details. Energetic considerations are of course of primary importance, in particular as concerns the activation energy for the dissociation, the stability of the dissociated with respect to the undissociated molecule (the process results in fact endothermic by 19 kcal/mol), the energy required for the singlet–triplet transition, and the stability of the trapped electron in the color center. All energies reported in the following are estimated at an HF level and do not include either the long-range polarization or the electron correlation correction.<sup>13</sup> The latter makes an important contribution to energy, but our previous work indicates that it should not affect very much energy differences between stable configurations of the kind considered here; its main effect is probably to lower the energy barrier for dissociation.

Much attention will also be given to the electronic structure of the different steps of the process; in particular, the electron spin density data of the paramagnetic state will be analyzed and compared with those obtained from previous theoretical calculations<sup>8–10</sup> and from the simulation of EPR experimental data.<sup>9</sup>

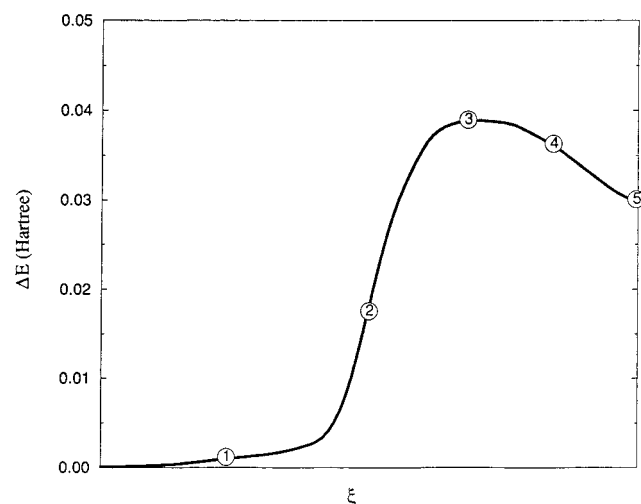


**Figure 2.** Energy versus  $\xi$  (the reaction coordinate) for the process of  $H_2$  dissociation. The numbers along the curve identify some intermediate configurations of interest represented in Figure 3.

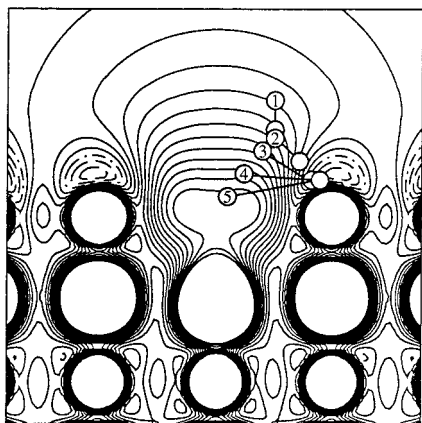


**Figure 3.** Electrostatic potential map for the relaxed anion vacancy with no trapped electrons and identification of the  $H_2$  dissociation path. The section is through the surface oxygens at the corners of the vacancy. Consecutive isopotential lines differ by 0.02 au (0.54 V); continuous, dashed, and dot-dashed curves refer to positive, negative, and zero potential, respectively. Lines corresponding to absolute values larger than 0.3 au are not plotted. Subsequent configurations of the two hydrogen atoms along the reaction path are identified. The corresponding energies are reported in Figure 2.

## 2. Results and Discussion

**A. Heterolytic Dissociation of the Hydrogen Molecule.** The identification of the reaction path for the  $H_2$  dissociation has required considering more than 100 configurations. The two hydrogen atoms have been allowed to move in the vertical plane through two oxygen atoms at opposite corners of the vacancy (see Figure 1), while leaving the geometry of the substrate fixed at the equilibrium configuration for the  $F_s^{2+}$  center (the surface anion vacancy with no trapped electrons).<sup>10</sup> Only in a final step the magnesium ions nearest to the vacancy were allowed to relax. The structure possesses only a plane of symmetry, and the computations are very expensive. We have tried both restricted and unrestricted HF calculations, but in all cases the restricted solution was the most stable. The results are shown in Figure 2. For the sake of the following discussion, the map of the electrostatic potential at the  $F_s^{2+}$  center is reported in Figure 3; subsequent configurations of the dissociating molecule are here represented, and their energies are given in Figure 2.

The molecule approaches the surface in an upright position pointing to a location intermediate between a corner oxygen

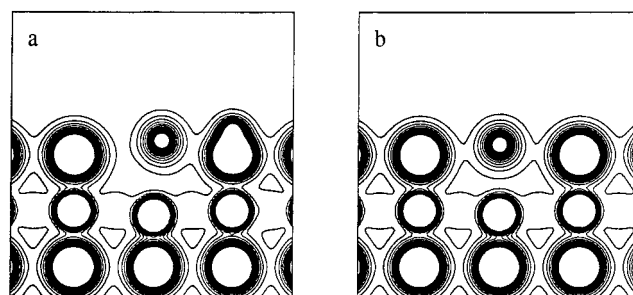


**Figure 4.** Total electron density maps for the adsorbed dissociated molecule (a) and for the isolated hydride ion (b) at the vacancy. The section is the same as in Figure 3. A linear scale has been employed with isodensity values differing by 0.01  $|e|/\text{Bohr}^3$ . Lines corresponding to densities larger than 0.15  $|e|/\text{Bohr}^3$  are not drawn.

and the center of the vacancy. At about 2 Å from the surface, the electrostatic field is sufficiently strong to polarize the molecule and to attract the lower H atom toward the oxygen. The distance between the two hydrogens is progressively increased and the polarization enhanced; this phase of the process corresponds to the top of the energy curve: the energy barrier is 0.04 Hartree or 25 kcal/mol. The two ionic fragments now follow the lines of the electrostatic field and finally reach the configuration of the precursor state, which is unstable by 19 kcal/mol with respect to the initial state (the isolated  $H_2$  molecule plus the  $F_s^{2+}$  center).

The activation energy is too large to be compatible with the experimental observation that dissociation takes place rather fast at room temperature. Correlation corrections could decrease the present estimate of the barrier, but this should not change the above conclusion because the products themselves are much higher in energy than the reactants: on the contrary, recombination of the two atoms would become even easier. We believe that this disagreement with the experiment is due to the inadequacy of the model, not to inaccuracy of the calculations. Simply, the isolated anion vacancy at the perfect (100) surface is not capable of dissociating  $H_2$ . This result contrasts sharply with that obtained nearly 20 years ago by Colbourn and Mackrodt<sup>15,16</sup> who found the present reaction to be nonactivated and exothermic by 130 kcal/mol. The largest cluster used for that study included only the vacancy, its five nearest cations and the four next nearest anions, embedded in an array of classical point charges to simulate the (100) surface, while the two hydrogen atoms were allowed to move in a vertical line through the center of the vacancy. It is hard to believe that this oversimplified model (which finds its obvious justification in the state of the computer technology at that time) can properly reproduce the chemical activity of ions belonging to the crystalline lattice; furthermore, either the polarizability of  $H_2$  or the electrostatic field above the site was grossly overestimated. Therefore we consider their outcome as a computational artifact.

**B. Precursor State and Hydride–Vacancy Complex.** The structure of the precursor state, which is the dissociated molecule at the vacancy, is here compared with the similar case of the hydride–vacancy complex alone, in the absence of a vicinal hydroxyl. The corresponding equilibrium configurations are reported in the bottom left plot of Figure 1, while the electron densities are shown in Figure 4.

The bond length of the hydroxyl group is 0.955 Å, which is the standard value for this group; the proton is almost vertically above the oxygen. The HV complex near the hydroxyl resembles an elongated hydride ion, as shown by the density map; due to the attraction by the proton, the complex is slightly off-center



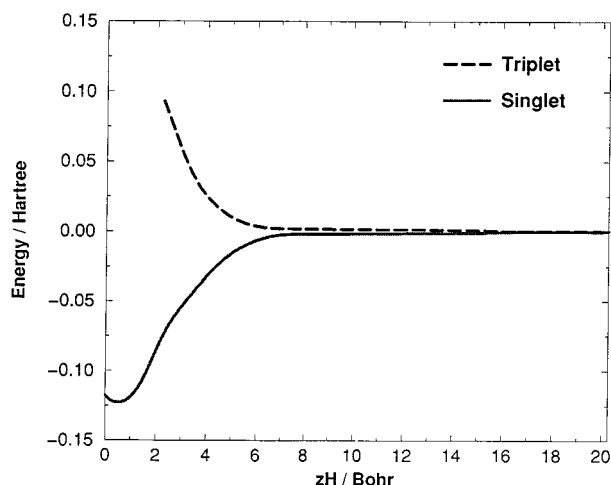


**Figure 5.** Energy versus distance from the surface of the fundamental and first-excited (triplet) state of the hydride-vacancy complex.

(0.5 Bohr). In the absence of the hydroxyl the situation is not changed very much: HV is obviously at the center of the vacancy, but its shape is similar to the previous one, and the proton is very close to the surface plane in both cases. The relaxation of the magnesium ions around the vacancy in the presence of the hydride is similar to that found for the paramagnetic  $F_s^+$  center (a surface vacancy with a trapped electron) and considerably less important than for the  $F_s^{2+}$  center (a surface vacancy with no trapped electrons).<sup>10</sup> The Mulliken charge of HV, obtained by summing the contributions of the functions centered on H and on the ghost atom, is the same in the two cases: 2.105 e.

**C. Dissociation of the Hydride-Vacancy Complex: Ground and First-Excited Triplet States.** In order to study the excitation of the HV complex, we chose to neglect the presence of the hydroxyl: the computations are much faster because a smaller cluster is needed (see Figure 1), and the local symmetry is much higher ( $C_{4v}$  instead of  $C_s$ ); the discussion above justifies this approximation.

Figure 5 reports the energy curves for the fundamental and first-excited (triplet) state as a function of the distance of the H atom from the surface plane, that is, of the elongation of the H-V bond. These curves look very similar, also from a semiquantitative point of view, to those of the textbook example of the homolytic dissociation of the  $H_2$  molecule (see, for example, refs 18 and 19); in both cases they converge to the same final situation consisting in an isolated hydrogen atom and in an electron at the vacancy.

Consider first the ground-state curve. This is obtained by connecting the restricted HF curve (corresponding to the most stable solution for distances up to 4 Bohr from the surface) with the UHF one (beyond 4 Bohr). The difference between the energy minimum and the energy at infinite separation between the hydrogen atom and the trapped electron is 0.130 Hartree, practically coincident with the binding energy of the  $H_2$  molecule calculated with the present basis set (0.1313 Hartree). On the other hand, as expected, the H-V bond is much softer than the H-H bond in the  $H_2$  molecule. From the curvature of the energy-versus-distance curve at the minimum, the wave-number for the vibration of the HV species is estimated at about  $900\text{ cm}^{-1}$ , or  $640\text{ cm}^{-1}$  for its deuterium analogue DV: this is about 1.4 factor smaller than experimentally observed ( $820\text{ cm}^{-1}$  for the bridged  $D^-$  species<sup>3</sup>).

The triplet solution is difficult to obtain when the hydride is at distances shorter than 2 Bohr from the surface. By extrapolat-

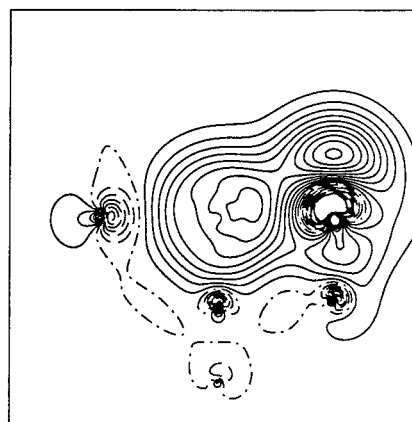


**Figure 6.** Plot of the HF orbital  $\psi_1(r)$  associated with the lone-electron state for the  $F_s^+(H)$  center in the same section as in Figure 3. Consecutive isoamplitude curves are separated by  $0.01\text{ }(|e|/\text{Bohr}^3)^{1/2}$ .

ing data at larger distances, the vertical singlet-to-triplet excitation energy is estimated at 0.28 Hartree or 7.6 eV; that is, it lies in the near UV. As soon as it forms, the excited species dissociates promptly in a trapped electron and a neutral H atom, which should be expelled at high speed from the surface rather than be captured at a nearby site. This finding seems to contrast with the experimental observation of the formation of new  $OH^-$  bands as a consequence of UV irradiation. However, the real situation is not one of an idealized planar surface, so the expelled H atom may well be captured at an adjacent crystal grain.

**D. Trapped Electron Near a Hydroxyl Group: Final State.** We now consider the final situation, where an electron has remained trapped in the vacancy near a hydroxyl group. This geometric arrangement has been studied along with a variety of other hypothetical structures of the  $F_s(H)$  center by Giamello et al.,<sup>9</sup> using cluster models: in that case, the interest was centered on EPR parameters, rather than on energy data. The vacancy with an electron and no hydroxyls nearby has also been investigated theoretically.<sup>8,10</sup> The results of these previous studies are compared below with the present ones.

In order to properly describe the interaction of the electron with the hydroxyl, which has important consequences on the distribution of spin densities, we have used again the larger cluster with reduced symmetry. All these calculations have been performed in the UHF approximation. The equilibrium geometry, shown in Figure 1, almost coincides with that of the precursor state, which shows that the trapped electron plays a role very similar to that of the hydride as concerns the relaxation of the neighboring ions. However, the distribution of the lone electron is by far more sensitive to external fields than that of the hydride. To clarify this point, let us consider the defect state  $\psi_1(r)$ , with eigenvalue  $\epsilon_l = -0.362$  Hartree, which contains the unpaired  $\alpha$  electron. It is interesting to observe that this level is *below* the top of the valence band ( $-0.340$  Hartree in the host crystal). This apparent paradox finds its explanation in the fact that the high positive charge ( $+2\text{ }|e|$ ) at the defect region lowers locally the crystal bands (similarly to the band-bending effect in the physics of semiconductors). In fact, in the local region, the top of the valence band is at  $-0.477$  Hartree and  $\psi_1$  does not mix with states in the continuum. The distribution of  $\psi_1$  reported in Figure 6 reveals that the lone electron is strongly attracted by the proton of the hydroxyl. Since the spin density  $\rho_s(r)$  is almost entirely due to this state (the spin polarization of the other orbitals is very small) it is not surprising that much higher values of  $\rho_s$  are found at the two Mg nuclei closest to the hydroxyl than on the others (see Figure 7).

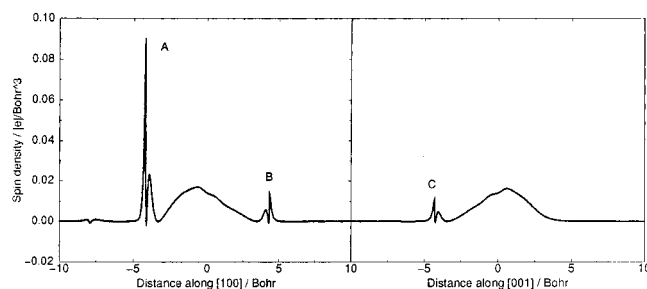


**Figure 7.** Linear plot of the spin density for the paramagnetic defect ( $|e|/\text{Bohr}^3$ ) along the (100) and (001) directions through the vacancy. The sharp maxima occur at the nuclei of first neighbor Mg ions. The distances from the defect center are in Bohr.

**TABLE 1: Calculated Values of the Spin Density  $\rho_s$  (au) at the Mg Nuclei Around the Trapped Electron<sup>a</sup>**

method (ref)	Mg <sub>A</sub>	Mg <sub>B</sub>	Mg <sub>C</sub>
Hydroxyl Present			
PC (present work)	0.0906	0.0133	0.0102
CIF (a: 18 atoms) (9)	0.131	0.014	0.028
CIF (b: 26 atoms) (9)	0.096	0.022	0.025
Hydroxyl Absent			
PC (10)	0.039	0.039	0.027
CIF (17 atoms) (8)	0.053	0.053	0.074
CIF (25 atoms) (8)	0.056	0.056	0.036
CIF (41 atoms) (8)	0.043	0.043	0.053

<sup>a</sup> The present technique is indicated as PC (perturbed cluster); the CIF ("cluster-in-field") technique utilizes a molecular cluster (whose size is indicated) extracted from the defective crystal and surrounded by an array of point charges. Labels for the nuclei are as in Figure 1. The coefficient for obtaining  $A_0$  (the isotropic hyperfine splitting constant for  $^{25}\text{Mg}$  nuclei, in Gauss) is 97.75. The experiment predicts two families of Mg nuclei, with spin densities 0.114 and 0.0076 au, respectively.

Table 1 compares the present results with those reported in previous papers. The agreement with the data obtained by Giamello et al.<sup>9</sup> is satisfactory, if account is taken of the dependence of the latter on the size of the cluster. The experimental data are also well-reproduced, in particular the observation that the higher spin density must be found not just on one but at least on two equivalent Mg nuclei. The role of the proton in determining the spin anisotropy is also evident: in its absence, the distribution of the spin at the five neighboring Mg ions is practically the same.<sup>8,10</sup>

### 3. Conclusions

On the basis of the energetics, the isolated surface anion vacancy is probably to be excluded as the site of formation and localization of the  $F_s^+(\text{H})$  center in polycrystalline MgO. On the other hand, this model seems adequate on many other

respects: IR vibrational frequency of the bridged adsorbed hydride, energy required for the generation of the paramagnetic species via a singlet–triplet transition, and features of the EPR spectrum. It is possible that this agreement is not coincidental: any local structure which can favor the formation of a hydride–proton pair at a distance of about 2.2 Å might exhibit a similar behavior. If it is so, the experimental evidence which seems to indicate that a topologically well-defined site is the host of the  $F_s^+(\text{H})$  center could instead be compatible with a variety of surface defects. Energetic and entropic considerations would then be of primary importance in determining their distribution. Work is in progress to characterize one of such candidate sites, namely, the *tub* divacancy (corresponding to the removal of a pair of adjacent surface ions), which has already been suggested to be a much more common defect than the isolated vacancy because of its lower formation energy and its charge neutrality.<sup>13</sup>

**Acknowledgment.** The present work is part of a project coordinated by A. Zecchina and cofinanced by the Italian MURST (Cofin98, Area 03). One of us (L.O.) is thankful to the European Community for a 6-month Training and Mobility of Researchers Marie Curie Research Grant (ERBFMBICT-961469). Financial support from the Italian CNR is also acknowledged. We are grateful to Silvia Casassa for her help in collecting the results described in the present work.

### References and Notes

- (1) Coluccia, S.; Boccuzzi, F.; Ghiotti, G.; Morterra, C. *J. Chem. Soc. Faraday Trans. 1* **1982**, 78, 2111.
- (2) Knözinger, E.; Jacob, K. H.; Hofman, P. *J. Chem. Soc. Faraday Trans. 1993*, 89, 1101.
- (3) Paganini, M. C.; Chiesa, M.; Giamello, E.; Coluccia, S.; Martra, G.; Murphy, D. M.; Pacchioni, G. *Surf. Sci.* **1999**, 421, 246.
- (4) Tench, A. J.; Nelson, R. L.; *J. Colloid Intef. Sci.* **1968**, 26, 364.
- (5) Tench, A. J. *Surf. Sci.* **1971**, 25, 625.
- (6) Giamello, E.; Murphy, D. M.; Ravera, L.; Coluccia, S.; Zecchina, A. *J. Chem. Soc. Faraday Trans. 1994*, 90, 3167.
- (7) Murphy, D.; Giamello, E. *J. Phys. Chem.* **1995**, 99, 15172.
- (8) Ferrari, A. M.; Pacchioni, G. *J. Phys. Chem.* **1995**, 99, 17010.
- (9) Giamello, E.; Paganini, M. C.; Murphy, D. M.; Ferrari, A. M.; Pacchioni, G. *J. Phys. Chem.* **1997**, 101, 971.
- (10) Scorza, E.; Birkenheuer, U.; Pisani, C. *J. Chem. Phys.* **1997**, 107, 9645.
- (11) Lunsford, J. H.; Jayne, J. P. *J. Phys. Chem.* **1996**, 70, 3464.
- (12) Lunsford, J. H. *J. Phys. Chem.* **1964**, 68, 2312.
- (13) Ojamäe, L.; Pisani, C. *J. Chem. Phys.* **1998**, 109, 10984.
- (14) Pisani, C.; Birkenheuer, U.; Corà, F.; Nada, R.; Casassa, S. *EMBED96 User's manual*; Università di Torino: Torino, 1996.
- (15) Colbourn, E. A.; Mackrodt, W. C. *Surf. Sci.* **1982**, 117, 571.
- (16) Colbourn, E. A. *Rev. Solid State Sci.* **1991**, 5, 91.
- (17) Kobayashi, H.; Yamaguchi, M.; Ito, T. *J. Phys. Chem.* **1990**, 94, 7206.
- (18) Pilar, F. L. *Elementary Quantum Chemistry*; McGraw-Hill: New York, 1968; pp 485 ff.
- (19) Szabo, A.; Ostlund, N. S. *Modern Quantum Chemistry*; Dover: New York, 1989; pp 221 ff.